



# Synthesis of Oxide Ceramics in Detonating Atmosphere

Pierre Gibot

## ► To cite this version:

Pierre Gibot. Synthesis of Oxide Ceramics in Detonating Atmosphere. *Ceramics*, 2021, 4 (2), pp.249-256. <10.3390/ceramics4020019>. <hal-03365210>

**HAL Id: hal-03365210**

**<https://hal.science/hal-03365210v1>**

Submitted on 5 Oct 2021

**HAL** is a multi-disciplinary open access archive for the deposit and dissemination of scientific research documents, whether they are published or not. The documents may come from teaching and research institutions in France or abroad, or from public or private research centers.

L'archive ouverte pluridisciplinaire **HAL**, est destinée au dépôt et à la diffusion de documents scientifiques de niveau recherche, publiés ou non, émanant des établissements d'enseignement et de recherche français ou étrangers, des laboratoires publics ou privés.



HAL Authorization

# Synthesis of oxide ceramics in detonating atmosphere

Pierre GIBOT

Laboratoire des Nanomatériaux pour Systèmes Sous Sollicitations Extrêmes (NS3E), ISL-CNRS-UNISTRA UMR 3208, Institut franco-allemand de recherches de Saint-Louis (ISL), 5 rue du Général Cassagnou, BP70034, 68301 Saint-Louis, France.

**Abstract:** A detonation process based on 2,4,6 trinitrotoluene (TNT), used as an energetic reagent, was successfully implemented in the synthesis of a series of metal oxide ceramics. TNT offers better physicochemical and mechanical properties than the energetic compounds traditionally used in such processes, thus offering safer handling and transport conditions. The experimental procedure, which consisted to of mixing the energetic molecule with a ceramic salt, was simple to perform. The detonation products were characterized by X-ray diffraction, scanning and transmission electron microscopies, energy dispersive X-ray spectroscopy and nitrogen physisorption. The as-synthesized ceramic powders ( $\text{CeO}_2$ ,  $\text{HfO}_2$ ,  $\text{Nb}_2\text{O}_5$ , and  $\text{In}_2\text{O}_3$ ) were crystalline and made of nano-sized quasi-spherical particles. This investigation provides an enhanced detonation synthesis process for elaborating ceramics. The majority of the oxide materials mentioned in this study had never been prepared by the detonation process before.

**Keywords:** Explosion synthesis; TNT;  $\text{CeO}_2$ ,  $\text{HfO}_2$ ;  $\text{Nb}_2\text{O}_5$ ,  $\text{In}_2\text{O}_3$ .

---

## 1. Introduction

An explosion or detonation is a powerful, high-temperature ( $>1000^\circ\text{C}$ ) decomposition chemical reaction that releases a large amount of heat and pressure (GPa), as well as a large volume of gases, in a few microseconds [1]. Explosives, molecules that detonate, are most of the time used as a destructive source by the military (e.g., bombs, warheads, ammunition) or for civil engineering (e.g., road construction, mining, comminuting, avalanche maintenance, hazardous land stabilization, etc.). High-tech fields such as the exploration of space or in-orbit placement of satellites by means of launchers are also significant consumers of explosives [1].

In the 1960s, explosion or detonation was used to synthesize materials—in particular,  $\text{sp}^3$ -hybridation carbon phases like diamonds (ND) [2]. Nano-sized NDs were thus collected in the detonation soot after the detonation of a 2,4,6 trinitrotoluene/1,3,5 trinitro-1,3,5-triazine (TNT/RDX) mixture. Other carbon structures like nanotubes (NTs) were successfully synthesized by explosion from an energetic mixture based on 2,4,6-trinitrophenol (TNP), paraffin, and benzene at the beginning of the 2000s [3]. The detonation process was also implemented to create ceramic materials as oxides or, in a few cases, carbide

materials [4]. Single ( $\text{Al}_2\text{O}_3$ ,  $\text{ZrO}_2$ ,  $\text{TiO}_2$ , etc.) and mixed ( $\text{LiMn}_2\text{O}_4$ ,  $\text{MnFe}_2\text{O}_4$ ,  $\text{SrAl}_2\text{O}_4$ , etc.) oxides were thus synthesized from energetic charges made of RDX or ammonium nitrate (AN,  $\text{NH}_4\text{NO}_3$ ) as detonative compounds mixed with metallic salts as ceramic sources [5–15]. More recently, TNT molecule was offered as explosive source to synthesis zirconia nanopowder from polymer-coated zirconium sulfate tetra hydrate and pure silicon carbide (SiC) nanoparticles were prepared by the detonation of a TNT/RDX energetic charge previously mixed with a preceramic polymer (polycarbosilane) [16,17].

Herein, a series of transition metal oxide ceramics were successfully synthesized by using the detonation process. Trinitrotoluene (TNT), a secondary explosive molecule, was used as the energetic source. Compared to the energetic materials most often used in such an approach, i.e., AN and RDX compounds that exhibit a high chemical sensitivity toward metallic species [18] and higher sensitivities to mechanical stimulus [19], respectively, the TNT molecule can be seen to be a safer alternative and of highest interest. In addition in the present investigation, the experimental procedure has been significantly revised compared to [16] in order to drastically reduce the number of steps and then make it easier to implement. Two main changes, highly time-consuming, were thus made, namely the removal of the use of a polymer additive (coated on the surface of the metal salt particles before mixing with the explosive molecule to avoid possible friction phenomena between ceramic and explosive particles during pressing step) and the temperature-controlled hydraulic pressing step which was replaced by a manual encapsulating of the as-prepared energetic mixture in a plastic tube (before detonation experiment). To date, to the best of our knowledge, the synthesis by detonation of  $\text{HfO}_2$ ,  $\text{Nb}_2\text{O}_5$ , and  $\text{In}_2\text{O}_3$  ceramics has not been reported. These ceramic oxides, in particular those based on niobium and indium, have been selected for their potential interest as oxidizers in the formulation of metal/oxide ceramic energetic composites (i.e., thermites) [20,21]. Over the last two decades, these energetic materials have attracted increasing attention in pyrotechnics due to the use of nanopowders that significantly improve their intrinsic performance (ease of ignition, increased burning rate...) [22].

## 2. Materials and Methods

The 2,4,6 trinitrotoluene (TNT,  $\text{C}_6\text{H}_2(\text{NO}_2)_3\text{CH}_3$ ) explosive molecule was purchased from Eureenco (Sorgues, France). Cerium sulfate tetra hydrate ( $\text{Ce}(\text{SO}_4)_2 \cdot 4\text{H}_2\text{O}$ , 98+%), hafnium dichloride oxide octahydrate ( $\text{HfOCl}_2 \cdot 8\text{H}_2\text{O}$ , 98+%), niobium (V) oxalate hydrate ( $\text{C}_{10}\text{H}_5\text{NbO}_{20} \cdot x\text{H}_2\text{O}$ , 99%), and indium (III) acetate ( $\text{In}(\text{OOCCH}_3)_3$ , 99.99%) were obtained from Alfa Aesar (Ward Hill, MA, USA). Heptane ( $\text{C}_7\text{H}_{16}$ , reagent grade) was obtained from Prolabo (Paris, France). Chemicals were used without further purification.

The experimental procedure conducted in this investigation was as follows: 225 g of TNT explosive molecule was mixed with 25 g of ceramic salt (90:10 wt. %) in 250 mL of heptane. The suspension was filtrated and the solid phase dried at 70 °C for 12 h. The resulting dry powdered mixture (230 – 250 g) was placed in a polypropylene tube ( $\varnothing = 43$  mm,  $L = 150$  mm). A booster (graphite/wax/1,3,5-trinitro-1,3,5-triazinane secondary explosive (RDX), 0.5/5/94.5 wt. %,  $m = 55$  g,  $\varnothing = 28.4$  mm,  $L = 57.5$  mm)

and a non-electric initiator (Titanobel) were added, to the tube containing the TNT/ceramic salt mixture, in order to achieve an energetic train (Figure 1A). A booster was placed between the non-electric initiator and the energetic charge to get a reliable initiation and propagation of a stable detonation within the TNT/ceramic salt mixture. On the basis of our own experiments, the 90:10 wt.% ratio of explosives and ceramic salts is considered as a good compromise, since a charge richer in ceramic salts produces a larger amount of material but with a larger particle size, whereas a charge richer in explosives synthesizes smaller particles but in greatly reduced quantities. The loading density was about 1.138 g/cm<sup>3</sup>, 1.098 g/cm<sup>3</sup>, 1.053 g/cm<sup>3</sup> and 1.094 g/cm<sup>3</sup> corresponding to a theoretical maximum density (TMD) of 65%, 64.9%, 63.3% and 64.5%, for the TNT/Ce, TNT/Hf, TNT/Nb and TNT/In mixture, respectively. The energetic train was placed in a volume of demineralized water (3 L, cooling medium for detonation products) and placed at the centre of a detonation chamber (Figure 1B) before the reaction took place. The detonation experiments were triggered by connecting the detonation cable of the non-electric initiator to a specific device capable of generating a high-energy, high-temperature spark. Finally, a purification process (filtration, oxidizing heat treatment (650 °C, 30 min) and acid etching (hydrochloric acid 2M)) was performed to collect the as-detonated ceramic material of the detonation soot.

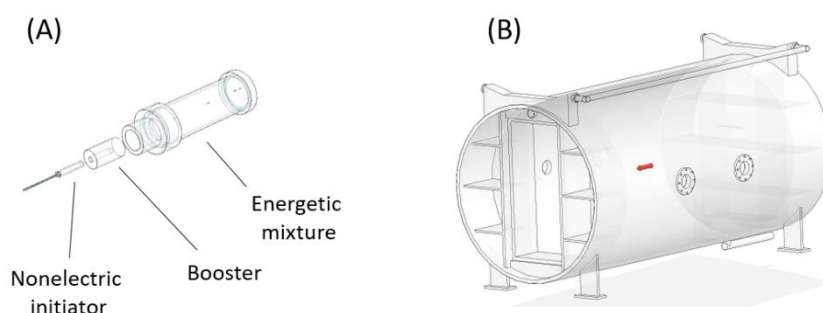


**Figure 1.** The energetic train (A) and the detonation chamber (B) used for the synthesis of oxide ceramics. The red cylinder in the detonation chamber represents the energetic train.

The structure and microstructure of the as-detonated materials were investigated by means of an X-ray diffractometer (XRD, D8 Advance, Bruker, Billerica, MA, USA) and a scanning and transmission electron microscopes (SEM-Nova NanoSEM 450 and TEM-CM200, FEI, Hillsboro, OR, USA), respectively. The textural properties (specific surface areas, pore volumes) of the powders, degassed at 200 °C for 6 h, were determined by nitrogen adsorption measurements at 77K (ASAP 2020, Micromeritics, Norcross, GA, USA). Specific surface area (SSA) were determined by taking into account the Brunauer–Emmett–Teller (BET) theory in the relative pressure range of  $p/p_0 = 0.05 - 0.25$  and the pore volumes were measured at  $p/p_0 = 0.99$ .

### 3. Results

Figure 1 shows the XRD patterns of the different ceramics synthesized by detonation. The diffraction peaks of patterns A to D were attributed to cerium (IV) oxide (CeO<sub>2</sub>, cubic structure, Fm-3m (225) space

group), hafnium (IV) oxide (HfO<sub>2</sub>, monoclinic structure, P2<sub>1</sub>/a (14) space group), niobium (V) oxide (T-Nb<sub>2</sub>O<sub>5</sub>, orthorhombic structure-Pbam space group), and indium (III) oxide (In<sub>2</sub>O<sub>3</sub>, cubic structure, Ia-3 (206) space group), respectively. The Miller planes were reported on the corresponding diffraction peaks, taking care to maintain the readability of the patterns. The removal of any amorphous carbon phases were systematically verified by thermo gravimetric analyses (not shown here).

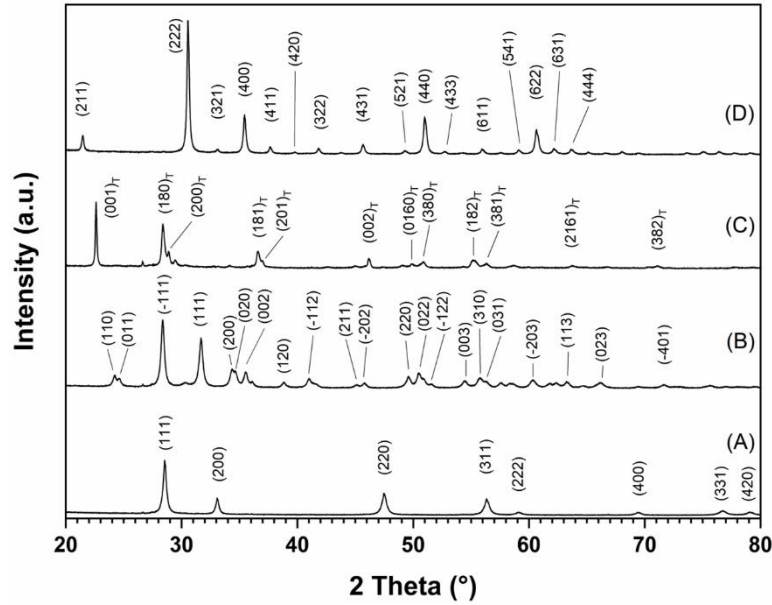


**Figure 2.** XRD patterns of the as-detonated oxide ceramics: (A) CeO<sub>2</sub> (JCPDS card No. 01-081-0792), (B) HfO<sub>2</sub> (JCPDS card No. 00-034-0104), (C) Nb<sub>2</sub>O<sub>5</sub> (JCPDS cards No. 00-30-0873), and (D) In<sub>2</sub>O<sub>3</sub> (JCPDS card No. 00-006-0416), respectively.

The coherence lengths or crystallite size (*L*) of oxide materials were determined using the Scherrer equation (1):

$$L_{hkl} = k \times \lambda / (\beta \times \cos\theta_{hkl}) \quad (1)$$

with *k* a dimensionless constant (0.89),  $\lambda$  the wavelength of the X-ray radiation ( $\lambda_{Cu}$ ),  $\beta$  the line broadening at full width at half maximum intensity (FWHM, corrected by the instrumental line broadening) and  $\theta$  the Bragg angle of the considered (*h,k,l*) Miller plane. Taking into account the most intense diffraction peak; namely the (111), (-111), (001) and (222) peaks for the CeO<sub>2</sub>, HfO<sub>2</sub>, Nb<sub>2</sub>O<sub>5</sub> and In<sub>2</sub>O<sub>3</sub> materials, respectively, coherence lengths were determined equal to 29 nm, 25 nm, 43 nm and 36 nm for the respective materials.

The microstructure (morphology and size) of the oxide ceramics was examined by scanning electron microscopy (SEM). The ceramic materials consist of micron-sized particles (< 1  $\mu$ m) coated by a plethora of smaller ones (Supplementary Materials). Representative views of this second population of particles (majority in number) are presented on magnified pictures in Figure 3 (top) for CeO<sub>2</sub>, HfO<sub>2</sub>, Nb<sub>2</sub>O<sub>5</sub>

and  $\text{In}_2\text{O}_3$ . The particles exhibit a quasi-spherical morphology with a size lower than 50 nm regardless the material considered. The particle size distributions of the different samples could not be determined by dynamic light scattering measurements because of the polydispersity of the samples (micro- and nano-particles).

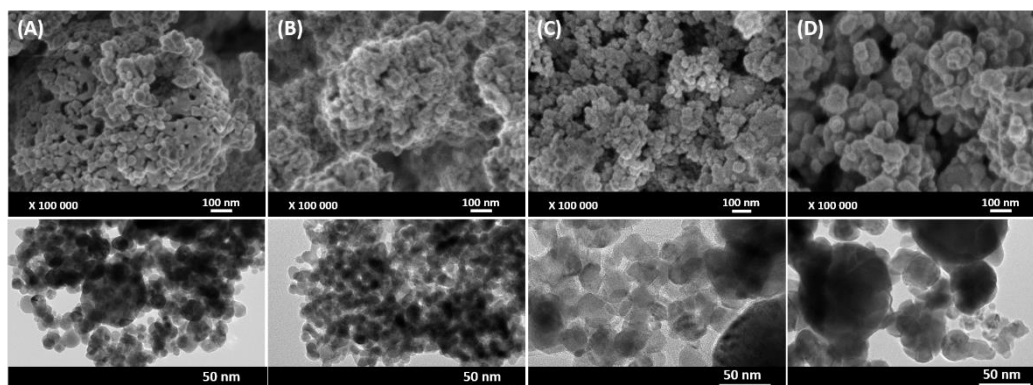


**Figure 3.** SEM (top) and TEM (down) images of the as-detonated (A)  $\text{CeO}_2$ , (B)  $\text{HfO}_2$ , (C)  $\text{Nb}_2\text{O}_5$ , and (D)  $\text{In}_2\text{O}_3$  oxide ceramics, respectively.

Additional characterizations by energy-dispersive X-ray spectroscopy supported the chemical nature of the as-detonated products (all kind of particles) since only the cerium, hafnium, niobium and indium metals and oxygen were identified on the different elemental mappings (Supplementary Materials). Traces of titanium, silicium, aluminum and iron originated from the set-up were also observed on particles bigger than  $1\text{ }\mu\text{m}$ . The four oxide materials were characterized by a transmission electron microscopy (TEM) analysis. At low magnifications, the images support the synthesis of oxide powders consisting of both micron ( $< \mu\text{m}$ ) and nanometer (largely dominant part) particles, as previously observed by SEM technique (Supplementary Materials). Representative images of nanoparticles are shown in Figure 3 (down). The size of these nanoparticles ranges from 20 to 50 nm, which is consistent with what was observed in the previous SEM characterization ( $< 50\text{ nm}$ ).

Nitrogen physisorption measurements were performed on the different oxide ceramics synthesized by detonation. The representative isotherms are displayed in Figure 4. According to the IUPAC standard, the four curves exhibit type-IV profiles with H3 hysteresis loops [23].

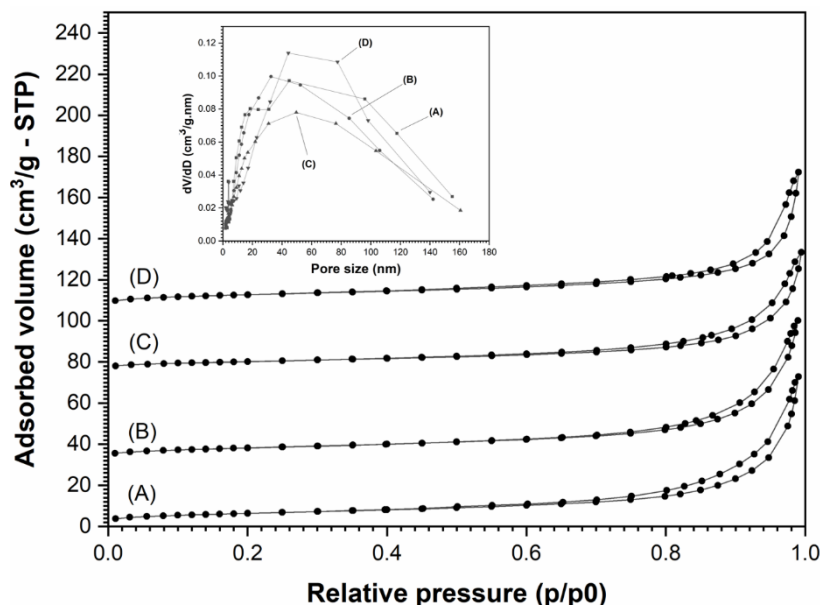


**Figure 4.** Nitrogen isotherms of the as-detonated ceramics: (A) CeO<sub>2</sub>, (B) HfO<sub>2</sub>, (C) Nb<sub>2</sub>O<sub>5</sub> and (D) In<sub>2</sub>O<sub>3</sub> materials, respectively. In insert, the corresponding particle size distributions.

Taking into account the BET model, specific surface areas of 22, 23, 28, and 20 m<sup>2</sup>/g were determined for the CeO<sub>2</sub>, HfO<sub>2</sub>, Nb<sub>2</sub>O<sub>5</sub>, and In<sub>2</sub>O<sub>3</sub> powders, respectively. Assuming dense, monodisperse and spherical particles, regardless of the chemical nature of the powder considered, the main particles' sizes ( $\varnothing$ ) were calculated by means of the formula (2) [23]:

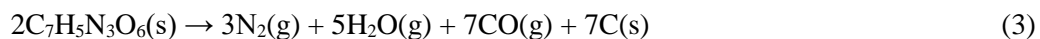
$$\varnothing = 6/(\rho \times \text{SSA}) \quad (2)$$

where  $\rho$  is the density (7.22, 9.68, 4.60, and 7.18 g/cm<sup>3</sup> for CeO<sub>2</sub>, HfO<sub>2</sub>, Nb<sub>2</sub>O<sub>5</sub> and In<sub>2</sub>O<sub>3</sub> oxide materials, respectively) and SSA the corresponding specific surface area. Average particle sizes of 37 nm, 27 nm, 46 nm, and 42 nm were thus calculated for the cerium, hafnium, niobium, and indium oxides, respectively. These data were consistent with the sizes observed by the SEM analysis for each material, especially for the smallest particles and thus confirm the high predominance of nano-sized particles (in volume) over micron-sized particles. Pore volumes at  $p/p_0 = 0.99$  were determined to be equal to 0.11, 0.10, 0.09, and 0.10 cm<sup>3</sup>/g for the CeO<sub>2</sub>, HfO<sub>2</sub>, Nb<sub>2</sub>O<sub>5</sub>, and In<sub>2</sub>O<sub>3</sub> materials, respectively. With respect to the hysteresis loops, characteristics of non-rigid aggregates [23], large mesopores are expected as no plateaus were observed at high relative pressure  $p/p_0$ . Pore size distributions (PSD), calculated from the Brunauer-Jarrett-Halenda (BJH) model applied to the desorption branches of the nitrogen isotherms, confirmed the existence of pores of large size ranging from 10 to 200 nm and corresponding to inter-particles porosity (Figure 4, insert).

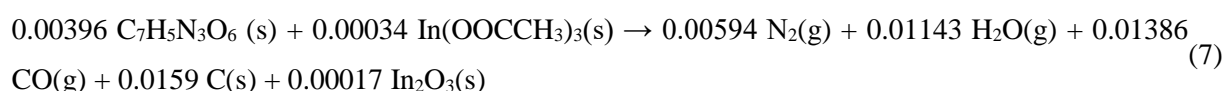
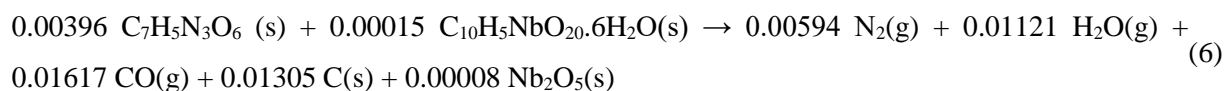
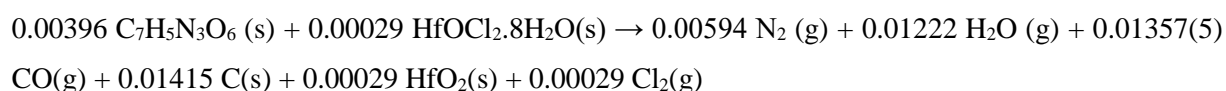
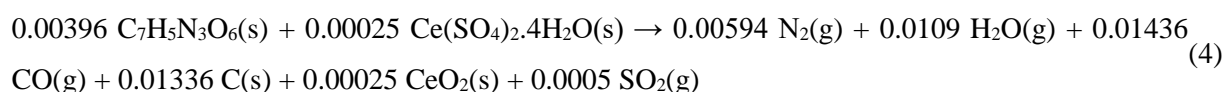
#### 4. Discussion

Based on the chemistry of explosives [24], the mechanism for the reaction taking place during the detonation process can be suggested. Conventionally, the explosive molecule, when it detonates, breaks

into the smallest possible entities such as atoms, which then leads to the formation of small stable inert species like nitrogen (N<sub>2</sub>), water (H<sub>2</sub>O), carbon mono/di-oxide (CO/CO<sub>2</sub>), etc. The nature and amount of the species strongly depend on the oxygen available within the explosive molecule considered. For instance, for the 2,4,6 trinitrotoluene molecule, in privileging the Kistiakowsky–Wilson rules [24], the decomposition reaction will be as follows:



This corroborates the above definition by supplying solid carbon phases since the oxygen present in TNT is not sufficient to completely oxidize the molecule. In fact, the oxygen balance, a factor that allows us to quantify the oxygen available to completely oxidize the considered molecule, is negative for the TNT compound (−77%). Now, considering a mixture of TNT with a ceramic salt (considered inert in the present investigation), the decomposition reaction of TNT will destroy the ceramic molecule and thus all atoms coming from the explosive and inert molecules will take part in the formation of detonation products. Accordingly, assuming 1 g of mixture (0.9 TNT/0.1 ceramic salt), the following global decomposition reactions can be offered:



In summary, carbon and oxide ceramic (CeO<sub>2</sub>, HfO<sub>2</sub>, Nb<sub>2</sub>O<sub>5</sub>, and In<sub>2</sub>O<sub>3</sub>) solid phases should be produced during the different detonation experiments. This hypothesis is consistent with the data obtained from the characterization techniques for all the detonation experiments above.

With regard to the particle size and shape of ceramic oxides synthesized by the detonation route, it is difficult to make a statement on the influence of just one specific parameter, as the detonation reaction is an extremely complex process involving decomposition, gasification and condensation reactions. However, the high pressures (GPa), the high temperatures (> 1000 °C) generated during detonation (μsec.) and the subsequent cooling rate (10<sup>9</sup> °C/sec.) play an undeniable role on the morphology and nanometric dimension of the materials thus prepared [1,2,24]. For example, for nanodiamonds (NDs)



synthesized by detonation of highly energetic explosives - and for which similar characteristics in terms of size (nm) and morphology are obtained - a mechanism of condensation of ultra-dispersed phases in a supersaturated gaseous phase combined with a rapid dispersion of the fluid environment (in a cooling medium) is suggested [25,26]. While the former affects the morphology, the latter is a key parameter for controlling the size of the particles produced. It can therefore be assumed that a similar mechanism occurs for the oxide materials prepared in the present study. Regarding the micron-sized particles found in all detonation soots, it can be speculated that their formation is due to several parameters such as the configuration of the charge (cylinder) as well as the porosity inside the charge (around of 35% assuming a loading density of 65% of the TMD) of the TMD for the different formulations) which can lead to the creation of zones where the generated temperatures and pressures are mitigated compared to the zones at the origin of the nanoparticle formation [5]. Therefore, the quenching of detonation products from these zones is not as drastic to control the growth of nanoscale particles and therefore the particles can grow. Another point could be the non-homogeneous dispersion of the ceramic salts in the energetic phase of TNT - creating inert phase micro-domains - which would fuel the growth of particles beyond the nanoscale. Currently, the concept of detonation synthesis, and more particularly the experimental parameters, are rethought in order to improve the current results because the fact that nano- and micro-particles coexist, can make it difficult to apply additional treatments.

## 5. Conclusions

Ceramic materials, i.e., cerium (IV) oxide, hafnium (IV) oxide, niobium (V) oxide, and indium (III) oxide, were synthesized by an explosion process. The insensitive 2,4,6 trinitrotoluene (TNT) explosive molecule was thus mixed with a ceramic salt (90:10 wt. %) in a non-polar solvent. After removal of the solvent, the resulting energetic charge was detonated in an aqueous medium to condense the detonation products. The experimental conditions resulted in the elaboration of crystalline ceramic powders with quasi-spherical particles of less 50 nm in size. This was the first report of the synthesis of  $\text{HfO}_2$ ,  $\text{Nb}_2\text{O}_5$ , and  $\text{In}_2\text{O}_3$  materials by means of this process. The present approach is expected to generate increasing attention in the preparation and scaling of nanomaterials, although improvements are needed to make such as-detonated samples reliable for a subsequent sintering process.

**Supplementary Materials:** The following are available online at [www.mdpi.com/xxx/s1](http://www.mdpi.com/xxx/s1), Figure S1: SEM (top) and TEM (down) low magnified images of pristine oxide ceramics: (A)  $\text{CeO}_2$ , (B)  $\text{HfO}_2$ , (C)  $\text{Nb}_2\text{O}_5$ , and (D)  $\text{In}_2\text{O}_3$ . Figure S2: Elemental mappings of the different calcinated as-detonated oxide ceramics: (A)  $\text{CeO}_2$ , (B)  $\text{HfO}_2$ , (C)  $\text{Nb}_2\text{O}_5$ , and (D)  $\text{In}_2\text{O}_3$ . The qualitative analyses were carried out by using a scanning electron microscope (SEM - JEOL JSM-7900F) equipped with an energy-dispersive X-ray spectroscopy device (EDS - Bruker Quantax XFlash® 6/30).

**Funding:** The author gratefully acknowledges the French National Centre for Scientific Research (CNRS), French German Research Institute of Saint-Louis (ISL, Saint-Louis, France) and University of Strasbourg (UNISTRA, Strasbourg, France) for funding.

**Acknowledgments:** The author acknowledges the French National Centre for Scientific Research (CNRS), the French German Research Institute of Saint-Louis (ISL, Saint-Louis, France) and the University of Strasbourg (UNISTRA, Strasbourg, France) for funding. The author also thanks L. Josien and L. Vidal (IS2M, Mulhouse-F), and C. Nicollet (ISL, Saint-Louis-F) for the transmission and scanning electron microscopy analyses and the formulation of the energetic charges, respectively.

**Conflicts of Interest:** The author declare no conflict of interest.

## References

1. Agrawal, J.P., High Energy Materials – Propellants, Explosives, Pyrotechnics, 1st ed.; Wiley-VCH: Weinheim, Germany, 2010.
2. Titov, V.M., Anisichkin, V.F., Mal'kov, I.Y. Synthesis of ultradispersed diamond in detonation waves. *Combust. Explos. Shock Waves*. **1989**, *25*, 372–379.
3. Lu, Y., Zhu, Z., Liu, Z. Catalytic growth of carbon nanotubes through CHNO explosive detonation. *Carbon*, **2005**, *42*, 361-370.
4. Cudzilo, S., Maranda, A., Nowaczewski, J., Trebinski, R., Trzcinski, W.A. Detonative synthesis of inorganic compounds. *J. Mater. Sci. Lett.* **2000**, *9*, 1997-2000.
5. Bukaemskii, A.A. Explosive synthesis of ultra-disperse aluminium oxide in an oxygen-containing medium. *Combust. Explos. Shock Waves*. **2001**, *37*, 594-599.
6. Li, R. Y., Li, X. J., Yan, H. H., Peng, J. Experimental Investigations of the controlled explosive synthesis of ultrafine Al<sub>2</sub>O<sub>3</sub>. *Combust. Explos. Shock Waves*. **2013**, *49*, 105-108.
7. Qu, Y., Li, X., Wang, X., Liu, D. Detonation synthesis of nanosized titanium oxide powders. *Nanotechnology*. **2007**, *18*, 205602-205607.
8. Qu, Y.D., Li, X.J., Yan, H.H., Ouyang, X. Selective synthesis of TiO<sub>2</sub> nanopowders. *Glass Phys. Chem.* **2008**, *34*, 637-639.
9. Yan, H., Zhao, T., Li, X., Zhao, B. Slurry explosive detonation synthesis and characterization of 10 nm TiO<sub>2</sub>. *Ceram. Int.* **2016**, *42*, 14862–14866.
10. Bukaemskii, A.A. Nanosize powder of zirconia. Explosive method of production and properties. *Combust. Explos. Shock Waves*. **2001**, *37*, 481-485.
11. Da Silva, C., Manuel, J., Dos Santos, A., Marisa, E. Nanometric-sized ceramic materials, process for their synthesis and uses thereof. United States Patent 8,557,215. 2013.
12. Dos Santos A., Marisa E., Da Silva C., Manuel J., Lagoa C., Cia A.L., Process for nanomaterial synthesis from the preparation and detonation of an emulsion, products and emulsions thereof. United States Patent 9,115,001. 2015.

- 276 13. Xie, X., Li, X., Zhao, Z., Wu, H., Qu, Y., Huang, W. Growth and morphology of nanometer  $\text{LiMn}_2\text{O}_4$   
277 powder. *Powder Technol.* **2006**, 169, 143-146.
- 278 14. Wang, X.H. Li, X.J., Yan, H.H., Xue, L., Qu, Y.D., Sun, G.L. Nano- $\text{MnFe}_2\text{O}_4$  powder synthesis by detona-  
279 tion of emulsion explosive. *Appl. Phys. A.* **2008**, 90, 417-422.
- 280 15. Li, X. Qu, Y., Xie, X., Wang, Z., Li, R. Preparation of  $\text{SrAl}_2\text{O}_4$ :  $\text{Eu}^{2+}$ ,  $\text{Dy}^{3+}$  nanometer phosphors by deto-  
281 nation method, *Mater. Lett.* **2006**, 60, 3673-3677.
- 282 16. Gibot, P., Vidal, L., Laffont, L., Mory, J. Zirconia nanopowder synthesis via detonation of trinitrotoluene.  
283 *Ceram. Intern.* **2020**, 46, 27057-27062.
- 284 17. Langenderfer, M.J., Fahrenholtz, W.G., Chertopalov, S., Zhou, Y., Mochalin, V.N., Johnson, C.E. Detona-  
285 tion synthesis of silicon carbide nanoparticles. *Ceram. Intern.* **2020**, 46, 6951-6954.
- 286 18. Medard, L. Les explosives occasionnels, 2nd ed. ; Lavoisier Techniques & Documentation : Paris, France,  
287 1999.
- 288 19. Meyer, R., Kohler, J., Homburg, A. Explosives, 6th ed.; Wiley-VCH: Weinheim, Germany, 2007.
- 289 20. Fischer, S.H., M.C. Grubelich. Theoretical energy release of thermites, intermetallics, and combustible met-  
290 als. Proceedings of the 32nd AIAA/ASME/SAE/ASEE Joint Propulsion Conference, Lake Buena Vista, FL, July  
291 1-3, 1996.
- 292 21. Gibot, P., Goetz, V. Aluminium/Tin (IV) oxide thermite composite: Sensitivities and reaction propagation.  
293 *J. Energ. Mater.* **2020**, 38, 295-308.
- 294 22. Pantoya, M.L., Granier, J.J. Combustion behavior of highly energetic thermites: Nano versus Micron com-  
295 posites. *Propellants, Explos. Pyrotech.* **2005**, 30, 53-61.
- 296 23. Lowell, S., Shields, J.E., Thomas, M.A., Thommes, M. Characterization of Porous Solids and Powders:  
297 Surface Area, Pore Size and Density, 1st ed.; Kluwer Academic Publishers: Dordrecht, The Netherlands, 2004.
- 298 24. Akhavan, J. The chemistry of explosives, 2nd ed.; Royal Society of Chemistry: London, United Kingdom,  
299 2004.
- 300 25. Dolmatov, V.Y. Detonation synthesis nanodiamonds: synthesis, structure, properties and applications. *Rus-*  
301 *sian Chemical Reviews.* **2007**, 76, 339-360.
- 302 26. Bastea, S. Nanocarbon condensation in detonation. *Scientific Reports.* **2017**, 7, 42151.